ACS APPLIED MATERIALS & INTERFACES

Research Article

www.acsami.org

Synthesis of Cytocompatible Luminescent Titania/Fluorescein Hybrid Nanoparticles

Kota Shiba,[†] Motohiro Tagaya,*[,‡] and Nobutaka Hanagata[§]

[†]World Premier International (WPI) Research Center, International Center for Materials Nanoarchitectonics (MANA), National Institute for Materials Science (NIMS), 1-1 Namiki, Tsukuba, Ibaraki 305-0044, Japan

[‡]Department of Materials Science and Technology, Nagaoka University of Technology, 1603-1 Kamitomioka, Nagaoka, Niigata 940-2188, Japan

[§]Nanotechnology Innovation Station, National Institute for Materials Science (NIMS), 1-2-1 Sengen, Tsukuba, Ibaraki 305-004, Japan

Supporting Information

ABSTRACT: Luminescent titania-fluorescein (FS) hybrid nanoparticles (NPs) were successfully synthesized by a sol–gel reaction of titanium alkoxide in the presence of octadecylamine using a fluidic reactor with a Y-type channel. The molar ratio of FS/Ti ratio was varied in the range from 1/1000 to 1/100 in order to obtain the hybrid NPs with the different luminescent behavior. The shape of the NPs is spherical and their sizes are 400 nm which is almost the same irrespective of the FS content, suggesting the different FS molecular states in one NP. We also demonstrated that the hybrid NPs exhibited a characteristic luminescence; the NPs with the higher and lower FS contents exhibited an enhanced luminescence in PBS and air, respectively, indicating that the FS states responded to the molecular environment. Through cytocompatible experiments using the NPs, it turned out that they had a high compatibility for fibroblasts. Therefore, the preparation of a series of the luminescent NPs with a tunable luminescence property was achieved. The results will lead to a guideline to determine a proper combination between material composition and an environment where they are used, being useful for biomedical applications.

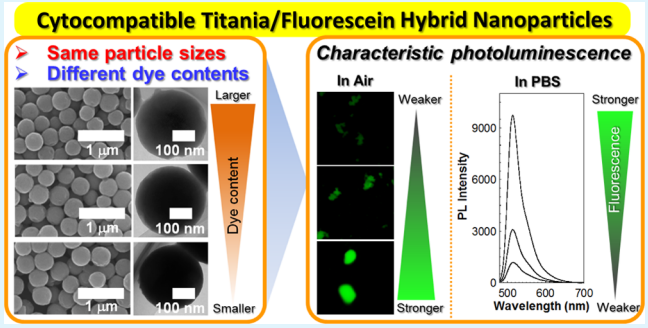

KEYWORDS: *titania, hybrids, fluorescein, bioimaging, nanomedicine*

INTRODUCTION

Targeting, bioimaging, and drug delivery to specific cell populations are key techniques in biomedical science fields. For advancing such fields, it is necessary to create hybrid nanomaterials, which have controlled particle size and shape. In particular, the monodispersed nanoparticles are useful as a model material, allowing to discuss their behavior in a human body. Additionally, it is also important to consider nanostructures of hybrids. The well-designed nanostructures make it possible to accommodate various species including surface functional groups, drug molecules, luminescent molecules, and so on. Among these species, luminescent ones, such as organic dye and quantum dots play an important role in realizing the biomedical applications because they can act as a biological probe.[1,2] The organic dyes are likely to be degraded by light exposure so that highly sensitive observation cannot be conducted. On the other hand, quantum dots are known as their sharp luminescence spectra where the luminescence wavelength can be tuned depending on the nanoparticle size. However, in most cases, quantum dots contain Cd, Hg, etc., which frequently cause some toxic effects. Therefore, it is expected to develop biocompatible and luminescent nanomaterials with a stable and characteristic luminescent property.

Hybrid functional nanomaterials have attracted many researchers because of their versatile properties. It is possible to combine various properties attributed to each component to overcome inherent drawbacks or improve specific abilities. Thus, a wide variety of hybrids have been reported with respect to their applications. There are major expectations that new functions are discovered through precise nanomaterial design. One of the most extensively studied hybrids would be inorganic–organic hybrid materials,[3−6] especially inorganic oxide-surfactant hybrids prepared by a surfactant-templated approach.[7] Since the inorganic oxide-surfactant hybrids are composed both of a hydrophilic oxide part and a hydrophobic organic part (alkyl chain of surfactant molecules) within their structures, they can solubilize hydrophobic molecules, such as dyes,[3,8−13] which is difficult for inorganic hydrophilic surfaces

Received: January 28, 2014
Accepted: April 14, 2014
Published: April 14, 2014

Scheme 1. Proposed Formation Process of the Titania-Based Hybrid NP Synthesis in This Study[a]

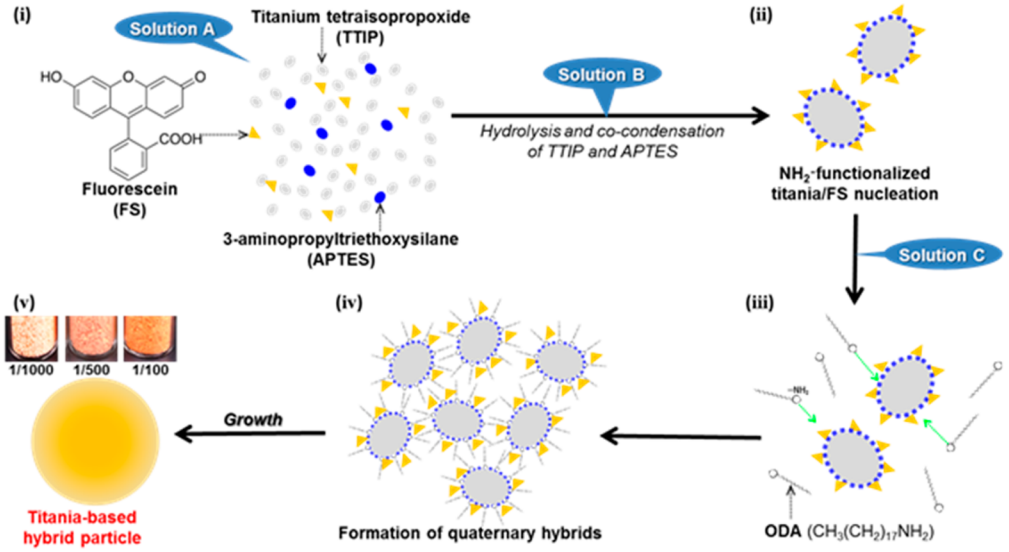

[a](i) TTIP, APTES and FS dissolve in IPA (Solution A), (ii) After admixing Solution A with Solution B (water/IPA admixture), TTIP and APTES are partially hydrolyzed to form NH_2-functionalized titania/FS nuclei, (iii) the pre-formed nuclei are admixed with Solution C that composed of water, IPA and ODA, resulting in the formation of NH_2-functionalized titania/FS/ODA hybrid nuclei, (iv) the hybrid nuclei assemble to form aggregates, and (v) the aggregates grow to form a spherical nanoparticle.

Table 1. Flow Rate and Chemical Components of the Solutions Used for the Synthesis of the Hybrid NPs

		solution A				solution B		solution C		
	flow rate ($mL \cdot min^{-1}$)	TTIP (mL)	APTES (mL)	fluorescein (mg)	IPA (mL)	IPA (mL)	H_2O (mL)	ODA (mg)	IPA (mL)	H_2O (mL)
*See SI	1.5	1.37	0.022	1.55	36.1	37.2	0.231	205	189	0.900
*See SI	7.5	1.37	0.022	1.55	36.1	37.2	0.231	205	189	0.900
*See SI	30	1.37	0.022	0.00	36.1	37.2	0.231	205	189	0.900
	30	1.37	0.022	1.55	36.1	37.2	0.231	205	189	0.900
	30	1.37	0.022	3.10	36.1	37.2	0.231	205	189	0.900
	30	1.37	0.022	15.5	36.1	37.2	0.231	205	189	0.900
	30	1.37	0.022	1.55	36.1	37.2	0.231	205	236	0.900
*See SI	30	1.37	0.022	1.55	36.1	37.2	0.231	205	236	3.00
*See SI	30	1.37	0.022	1.55	36.1	37.2	0.231	205	236	9.00

(e.g., bare silicas). This enables the oxide−surfactant hybrids to be utilized as a pigment, a laser emitter, etc., while further work is required to understand the resultant performance of the hybrids in more detail because the structure of the hybrids is complex due to the existence of multicomponents.

Since titania is a noncytotoxic material, its solubility in our body fluid is controllable. A large number of basic researches for the biomaterial applications have been performed utilizing oxide-based materials such as mesostructured silica,[14] dye containing silica,[15−17] silica coated quantum dots,[18,19] rare earth element doped silica[20−24] and so on. As related to these researches, the research for controlling the shape and NP size has been reported in terms of their synthetic techniques.[25−30] Furthermore, the formation of mesostructured titania has been reported.[31−34] Owing to its low solubility by light exposure, titania based luminescent nanomaterials have also been explored.[35−38] However, there are few studies on the cytocompatible luminescent titania based hybrid nanomaterials for the biomedical applications. For the sufficient conditions as biofunctional luminescent nanomaterials, the stability to light and thermal-exposure, longer excitation wavelength, non-cytotoxicity and nanometer size for the animal cell absorptions can be raised. Therefore, the development of titania based luminescent hybrid NP is of great importance.

To construct the specific properties of hybrid NPs, and to investigate their formation mechanism, they have to be precisely designed in terms of their size and shape. Monodispersed NPs help us to understand how homogeneous the composition of each hybrid NP is. We can then discuss the composition and the distribution of each component within one NP, closely related to the hybrid property that can provide various applications. In our previous study, a microfluidic device was successfully applied to separate the nucleation and growth processes which are important to obtain monodispersed products,[39−41] and titania-based monodispersed oxide-surfactant octadecylamine (ODA) hybrid spherical NPs were synthesized.[42,43] Taking advantage of the synthetic procedure, we now report the synthesis of fluorescein (FS)-containing monodispersed titania-ODA hybrid NPs with the same particle size and the different FS contents, as shown in Scheme 1. FS has been utilized in such fields as catalysis, optics, biology, and, especially, staining for living cell visualization. The titania-FS hybrids have attracted much attention because of its high stability and noncytotoxicity against the cells. Accordingly, it is worth investigating the way to prepare well-defined titania-FS

hybrids with controlled hybrid properties for biological functions. We also demonstrated the cytocompatible titania-ODA-FS hybrid NPs with a characteristic luminescence property for their nanoscale surface environment recognition.

EXPERIMENTAL SECTION

Materials. Titanium tetraisopropoxide (TTIP; Tokyo Chemical Industry Co., Ltd.), isopropyl alcohol (IPA; Wako Pure Chemical Industries, Ltd.), fluorescein (FS; Wako Pure Chemical Industries, Ltd.), octadecylamine (ODA; Aldrich, Inc.), 3-aminopropyltriethoxysilane (APTES; Sigma, Inc.), phosphate buffered saline (PBS; Invitrogen Co., Ltd., pH 7.4), fetal bovine serum (FBS; product no. 12603C, lot no. 6D0975, SAFC Bioscience Co., Ltd.), Dullbecco's minimum essential medium (DMEM; Invitrogen Co., Ltd.), ethanol (99.5 vol %, Wako Co., Ltd.), formaldehyde (37 vol %, Wako Co., Ltd.), and 0.05 w/v% trypsin−0.053 M ethylenediaminetetraacetate (trypsin-EDTA; No. 204-16935, Wako Co., Ltd.) were used. NIH3T3 fibroblasts (RCB1862) as a cell line were provided by the Riken BioResource Center. A plastic cell culture flask with an area of 75 cm^2 was purchased from BD Bioscience, U.S.A. All the reagents were used without further purification.

Sample Preparation. FS-containing titania-ODA hybrid NPs were synthesized based on a previously reported procedure.[42,43] The detailed conditions, such as composition of the starting solutions and flow rate, are summarized in Table 1. The experitimental equipment is schematically shown in Supporting Information Scheme S2. The admixture of TTIP, APTES, FS, and IPA (solution A) and aqueous IPA (solution B) were preparaed in glass vials. The two solutions were separately flowed into a PTFE tube (1 mm inner diameter) by a syringe pump (Fusion 200 Syringe Pump, provided by Chemyx, Inc.) at the flow rates of 1.5, 7.5, and 30 mL/min. The molar ratio of TTIP to H_2O in the admixture of the two starting solutions was set at 1/2.7 (Table 1). The two solutions were then admixed and reacted through the Y-shape junction of the flow reactor made of PTFE (the channel cross section of ∼1 mm^2, KeyChem mixer, YMC, Inc.). The admixture flowed through a PTFE tube of 70 cm in length. The admixture solution was then added to Solution C composed of H_2O, IPA, and ODA in a polypropylene bottle (the constatnt molar ODA/TTIP ratio of 0.18 (Table 1)) under stirring until the addition of the admixture was completed. After aging the solution at room temperature for 24 h, the product was separated by centrifugation (3500 rpm, 60 min), washed several times with IPA, and finally dried at 60 °C in air for 24 h.

To check whether FS molecules dissolve or not from the hybrid NPs in a biological fluid, 1 mL of PBS was added to each glass vial containing 10 mg of the resultant sample powder with the different FS content. After ultrasonication for 5 min, the vial was stationary standing at r.t. for 24 h. Finally, the dispersion was centrifuged (14500 rpm, 1 min) to collect the supernatant.

Characterization. Scanning electron microscope (SEM) images were obtained using a Hitachi Ultrahigh Resolution Scanning Electron Microscope SU8000 at an accelerating voltage of 10 kV. Prior to the measurements, the samples were coated with a few nanometers of platinum. The average particle size and coefficient of variation (CV) values were obtained from the SEM images by counting 100 particles. Transmission electron microscopy (TEM) was performed using a JEM-1400 (JEOL Co., Ltd.) at an accelerating voltage of 120 kV. Prior to the observation, the sample preparation was conducted by dispersing a small amount of the NPs into ethanol, casting the suspension on a carbon-coated copper grid, and then drying. The thermogravimetric-differential thermal analysis (TG−DTA) curves were recorded by a SII EXSTAR 6000 TG/DTA6300 at the heating rate of 10 °C/min under air flowing using α-alumina as the standard material. The photoluminescence properties were evaluated by photoluminescence spectroscopy. The excitation and luminescence spectra were recorded with the luminescence monitored at 548 nm for FS/Ti = 1/1000 at 555 nm for FS/Ti = 1/500 and at 568 nm for FS/Ti = 1/100, respectively, and at the excitation wavelength of 468 nm for the solid state measurement, and the excitation wavelength of 468 nm for the solution state measurement (excitation-slit/detection-slit: 5 nm/5 nm, measure time: 0.1 s, step width: 1.0 nm, sample weight = 150 mg). A fluorescent microscope (ECLIPSE Ni-E, Nikon) was utilized to obtain fluorescence images of the hybrid particles. For excitation, a wavelength of 465−495 nm was irradiated, and a wavelength of 515−555 nm was selectively focused on for the luminescence detection. The exposure time was 100 ms.

Scheme 2. Illustration of the Experimental Equipment That Contains the PTFE Fluid Channels for Synthesizing the Hybrid Particles

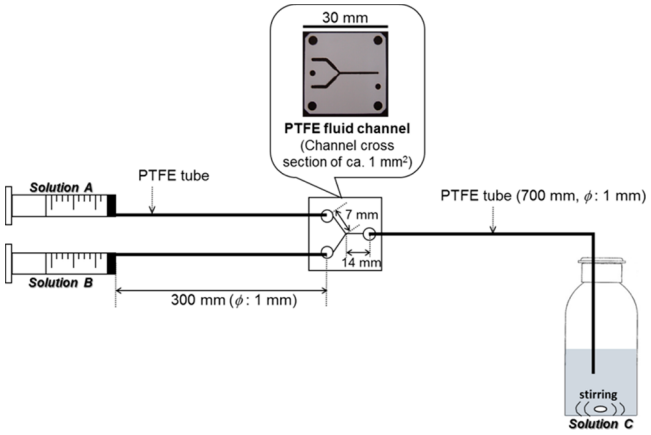

Cell Culture and Evaluation Method of Cytocompatibility. NIH3T3 fibroblasts (RCB1862) as cell lines provided by the Riken BioResource Center were cultured and used, then evaluated by the WST-8 method in this study.[20,44] On the basis of our previous report,[20,45] the fibroblasts were cultured in a plastic cell culture flask with an area of 75 cm^2 containing 15 mL of fetal bovine serum dispersed in DMEM at 10 vol % (10% FBS/DMEM). The cells were incubated at 37 °C in a humidified atmosphere of 5% CO_2, then subcultured every 7 days using 1 mL of the trypsin-EDTA. After being washed with 15 mL of PBS and treated with 1 mL of the trypsin-EDTA for 10 min at 37 °C, the cells were dispersed in 15 mL of PBS, separated by centrifugation (2000 rpm, 2 min), and dispersed in 15 mL of 10% FBS/DMEM. The centrifugation and dispersion were carried out twice. The number of cells in the suspension was counted and adjusted at the seeding density of 2.72×10^4 cells/mL. The fibroblast suspension was cultured on a commercially available 96-well cell culture plate at the area density of 8000 cells/cm^2. At the culture time of 12 h, 100 μL of the synthesized nanoparticles (NPs) in 10% FBS/DMEM (concentration = 100 μg/mL) was added to the cell surfaces and additionally cultured for 60 h according to our previous report.[46] At the additional culture times of 24, 36, and 60 h, the cell viability was evaluated by the WST-8 method. After washing the cellular surfaces, 10 μL of the Cell Counting Kit-8 solution was added and stored for 3 h at 37 °C in a humidified atmosphere of 5% CO_2. The absorbance at 450 nm of the resulting solution was measured by a photospectrometer. The background absorbance of the 10% FBS/DMEM was subtracted and the average value for ten samples was calculated. The absorbance maximum of the samples was 100%. The control, which was defined as the cells without adding the NPs, was used for the experiment.

For observing the cellular reactions, the cultured cells were fixed with 3.7 vol % formaldehyde in PBS for 10 min. Before and after the fixation, the cells were washed twice with 1 mL of PBS and twice with 1 mL of ultrapure water. Immediately, the cells in the PBS were covered and sealed with a glass to prevent evaporation with a confocal laser scanning fluorescence microscope (TCS SP-5, Leica Microsystems Inc.).

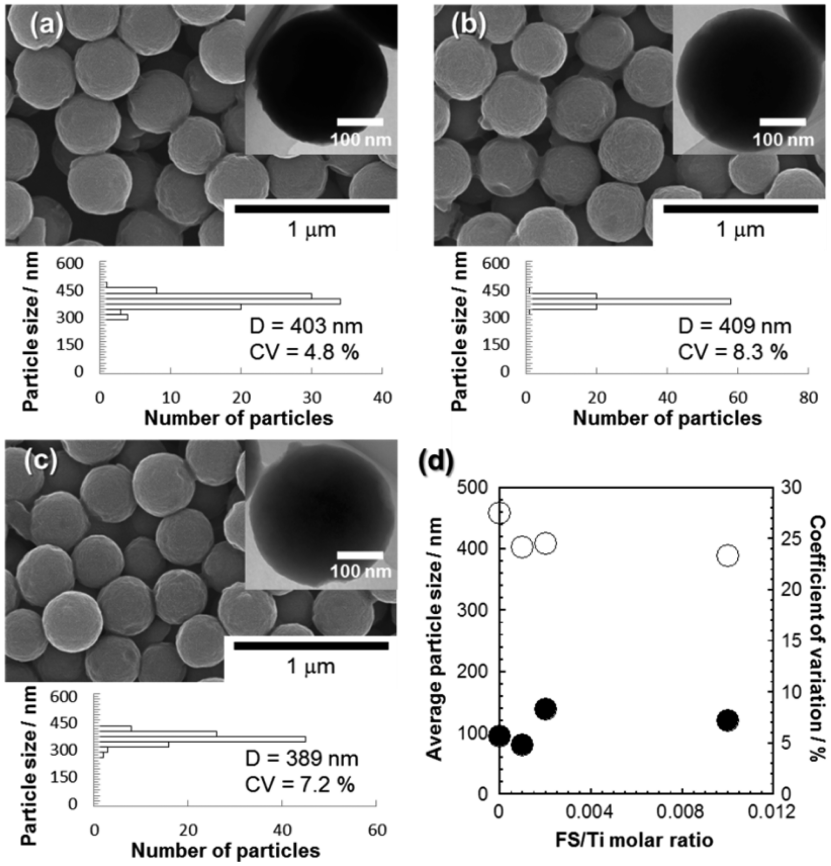

Figure 1. FE-SEM images and the corresponding particle size distributions of the hybrid NPs with the different FS/Ti molar ratios: (a) 1/1000, (b) 1/500, and (c) 1/100. The TEM images are shown in each inset. (d) The average particle size (open circle) and coefficient of variation (closed circle) changes with the FS/Ti molar ratio.

RESULTS AND DISCUSSION

Synthesis of Monodispersed Titania-ODA-FS Hybrid NPs. The separation of the nucleation and growth processes is important for the preparation of monodispersed NPs.[39−43] As we have already reported,[42,43] well-defined titania-ODA hybrid spherical NPs were synthesized by a two-step approach, in which nucleation occurs in the microfluidic reactor (solution A + B, without APTES and FS) and the nuclei were subsequently added to a reaction vessel (containing solution C) placed at the end of the reaction system for further growth. Taking advantage of the same technique, the hybrid NPs with three different FS contents, "i.e., molar ratios FS/Ti = 1/1000, 1/500, and 1/100" were synthesized in the present study. The synthesis proceeds based on the following two steps: formation of titania NPs by hydrolysis and condensation reaction of TTIP, and formation of titania-ODA hybrid NPs caused by several possible interactions, such as hydrogen bonding, hydrophobic interaction, etc. FS and APTES were both added to solution A in this study, expecting an interaction between the amino group of aminopropylsilane and carboxyl group of FS shown in Scheme 1i. The co-condensation of titania-ODA and various silane coupling reagents including APTES was also reported previously, and a homogeneous distribution of silyl groups in each NP was indicated.[47] Therefore, the present synthesis should lead to the formation of aminopropyl-functionalized monodispersed titania-ODA-FS hybrid spherical NPs as shown in Scheme 1iv. The reaction solution color turned orange and opaque in less than 1 min after admixing the three solutions. Orange colored powder was collected after 24 h as shown in Scheme 1v, which exhibits different colors depending on the FS concentration, indicating that the FS is included in the titania NPs.

SEM and TEM images of the collected products are shown in Figure 1. All the products were monodispersed with coefficient of variation ranging from 5% to 8%, which is the same as that of the control product synthesized without FS (Supporting Information Figure S1, as can be seen in each particle size distribution). Interestingly, all the three products showed almost the same NP size at around 400 nm in spite of the different FS amounts in solution A, while 460 nm in the case of the control without FS, indicating that different amounts of FS molecules interacted and were confined in the NP. Other control products were also prepared focusing on different synthetic parameters such as flow rate (Supporting Information Figure S2) and H_2O/IPA solvent ratio (Supporting Information Figure S3); the NP sizes were controlled in the range from 100 to 750 nm depending on the parameter. This implies the well-known particle size dependent cytotoxic effect, which are different from the purpose of only a surface effect in this study.

Discussion on the Formation Mechanism of the Hybrid NPs. One possible reason for the formation of the proposed formation mechanism as shown in Scheme 1. In Scheme 1i, TTIP, APTES, and FS coexist in solution A. The color of the Solution A turned from yellow to yellowish red after the addition of TTIP to the IPA solution containing APTES/FS, suggesting the TTIP-FS complex formation. It was pointed out that deprotonation of the hydroxyl group of

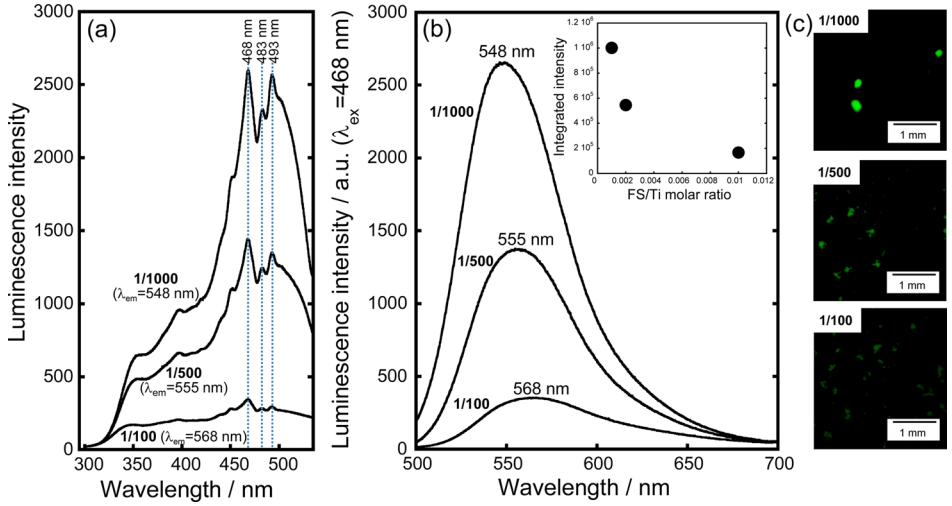

Figure 2. (a) Excitation and (b) luminescence spectra of the hybrid NPs with the different FS/Ti molar ratios of 1/1000, 1/500, and 1/100 (the excitation spectra were obtained for each luminescence maxima). Inset: the integrated intensity changes with the FS/Ti molar ratio. (c): Fluorescent microscope images of the hybrid particles with the different FS/Ti molar ratios (λ_{ex} = 465−495 nm, λ_{em} = 515−555 nm, exposure time = 100 ms).

fluorescein causes a red shift in the luminescence spectra. For example, the coordination of the hydroxyl group to titanium atoms presumably induces a similar red shift.[48]

After admixing solutions A and B, the hydrolysis and co-condensation reaction occurred, and the titania nuclei were partially modified with the aminopropyl groups (Scheme 1ii). The carboxyl groups of FS are thought to interact with the near-surface amino groups by an electrostatic interaction. In addition, it is known that carboxyl groups are also likely to bind to the titania surface through a dissociative process, which results in two oxygens of the carboxylate ion bonding to the in-plane titanium atoms at the interface. The remaining proton then bonds to a bridging oxygen site, forming a hydroxyl group.[49−51]

Subsequently, the preformed nuclei were added to solution C containing ODA to form titania-ODA-FS hybrids (Scheme 1iii−iv). It was pointed out that an amino group of ODA interacts with the titania surface hydroxyl groups by hydrogen bonding.[43,52] Furthermore, the ODA should also relate to the hydrogen bonding with a hydroxyl group in the FS molecular structure. After the formation of the aminopropyl-functionalized titania-ODA-FS nuclei, they grow to form a homogeneous spherical shape (Scheme 1iv−v). We have previously reported that the absence of ODA led to the formation of random-shaped NPs.[43] In addition, it turned out that ODA promoted the formation of the titania-based hybrid NPs with a yield at around 90%, while the titania yield was less than 50% without the ODA. On the basis of these results, the ODA molecules adsorb on the surface of the titania NPs, then the titania-ODA hybrids effectively assemble to form secondary NPs with spherical shape as shown in Scheme 1v, which may be initially driven by hydrophobic interactions. The main solvent of the present system is IPA and relatively smaller amount of H_2O molecules also coexist. Considering that IPA is hydrophilic and can freely admix with H_2O, hydrophobic ODA molecules are not easy to dissolve in IPA, although very small amount of ODA can dissolve (e.g., we experimentally checked that 0.2 g of ODA dissolved in 100 mL of IPA). H_2O molecules can form hydrogen bonding between IPA molecules as well as IPA−H_2O molecules, letting a propyl group of IPA molecules direct toward the alkyl chains of ODA molecules on the surface of the hybrid particles to stabilize the hybrids. When the hydrogen bondings are enhanced in the system, accelerating the precipitation of titania-ODA hybrids. We also checked that the ODA molecules in the hybrids did not dissolve into IPA even when the IPA was heated up to 70 °C, indicating that the interfacial interactions between titania and ODA is rather stable. This hypothesis can be supported by the fact that the higher molar water/IPA ratio in solution C resulted in the formation of the smaller sized NPs as shown in the Supporting Information Figure S3. This indicates that the hydrophobic titania-ODA NPs do assemble together if the water molecules increase more and more, and subsequently form the spherical shape in order to minimize the surface energy, suggesting the importance of the additive ODA in the synthesis.

In the present synthesis, the molar ODA/Ti ratio is 0.18, and the FS/Ti ratio is in the range from 0.001 to 0.01. This FS amount is not enough to cover the entire surface of the titania-based NPs if we take into account the surface area of the NPs with the size of 400 nm. We assume that both ODA and FS interact with the inside of the titania surface, leading to the three interactive hybrids (ODA-FS-titania) to be functionalized, although the orientation of ODA and FS is not clear. Therefore, the spherical NP formation should be dominated by ODA, and the constant ODA amount successfully gives the same hybrid NP size with the different FS contents, which can be regarded as a "surface effect". On the other hand, the reason for the slightly different NP sizes between the NPs synthesized with and without FS (400 and 460 nm, respectively) is now under investigation. The spherical NP formation may be possibly promoted because of the slightly hydrophobic near-surface properties as compared to the NPs without FS. This makes it possible to characterize and discuss the luminescence property in detail correlating with the nanoscale environment around the FS molecules in a NP.

Photoluminescence Property of the Hybrid NPs. The photoluminescence properties of the as-synthesized titania-ODA-FS hybrid NPs were characterized by fluorescent spectroscopy as shown in Figure 2, which was performed in atmospheric environment. In the excitation spectra (Figure 2a), there are three luminescence bands at 468, 483, and 493 nm. According to previous studies, the bands at 468 and 483 nm

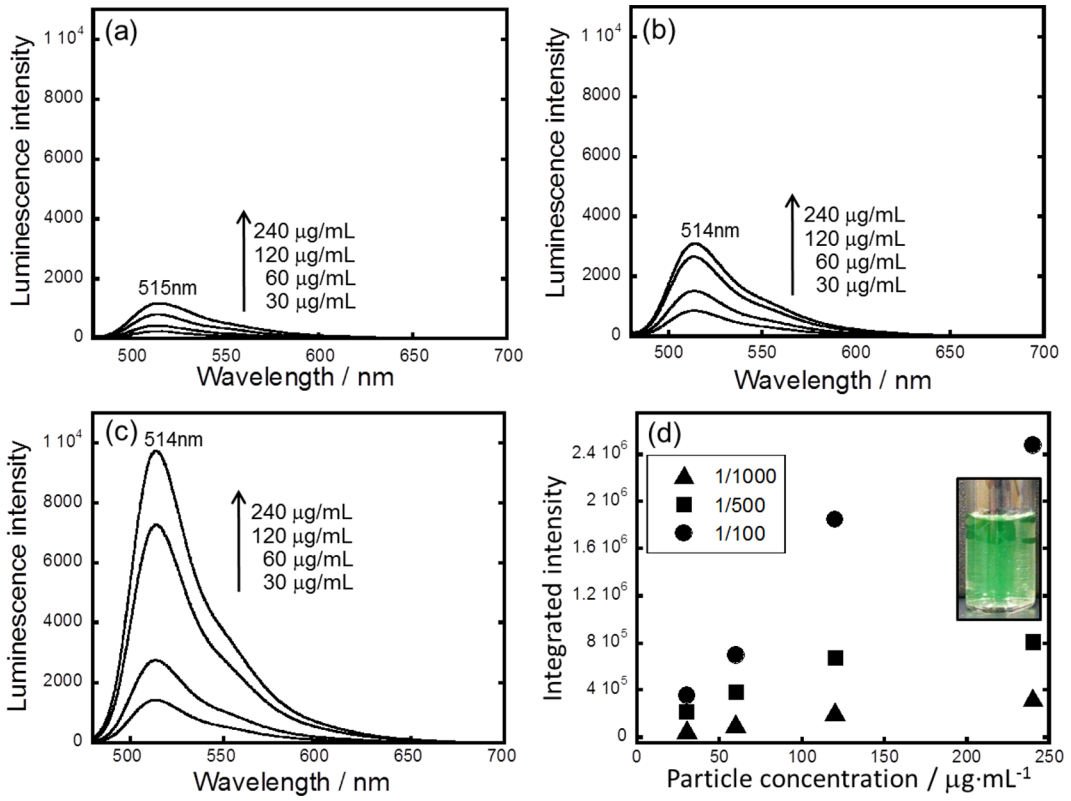

Figure 3. Photoluminescence spectra of the hybrid NPs with the different FS/Ti molar ratios of (a) 1/1000, (b) 1/500, and (c) 1/100 dispersed into PBS, and (d) the integrated intensity changes with the particle concentration. Inset: the photograph of the sample (FS/Ti = 1/100) dispersed into PBS under interior light at the concentration of 240 mg/mL, indicating the intense green luminescence.

can be attributed to the transition of the FS anion form, whereas the luminescence at 493 nm can be attributed to that of the FS dianion form,[53−55] suggesting the FS complex formation in the hybrids. As can be seen in each luminescence spectrum in Figure 2b, there is one luminescence band centered at around 550 nm. The luminescence appeared at around 520 nm is due to the monomer dianion states, whereas the luminescence appeared at around 560 nm, which is similar to that in the present study, is due to the FS aggregated states.[53] For more details, the spectral red shift with respect to the monomer was caused by the FS aggregation, in which the FS monomers were arranged in a head-to-tail manner (known as *J*-type aggregates). Moreover, this geometric restriction only allows a transition from the ground state to the lowest split level, causing the spectral red shift.[56] The luminescence integrated intensity decreases with the increasing molar FS/Ti, and the strongest luminescence was observed in the case of FS/Ti = 1/1000. This trend was also confirmed by observation using a fluorescent microscope as shown in Figure 2c; a bright green luminescence is clearly observed only in the case of FS/Ti = 1/1000, while the luminescence is relatively very weak in the case of FS/Ti = 1/100 (see also Figure S4 in the Supporting Information).

In addition to the luminescent behavior in air, we also characterized the luminescence in PBS virtually considering future experiments in body fluid. Before the photoluminescence measurements, we checked whether FS molecules dissolve or not from the hybrid NPs in PBS. TG-DTA curves of each sample are shown in the Supporting Information Figure S5, and the resultant weight loss values before and after PBS treatment in the range from 150 to 600 °C are summarized in the Supporting Information Table S1. The weight loss in this range can be attributed to oxidative decomposition of organic compounds (FS and ODA). There was no apparent weight loss after the PBS treatment of each sample (~a few wt % decrease), suggesting the slight dissolution of FS in PBS during the 24 h treatment. Furthermore, the hybrid NPs were dispersed in PBS at the NP concentration of 25−240 μg/mL, and the solution was aged at rt for 10 min, exhibiting no dissolution of FS at the shorter time.

Figure 3 shows the photoluminescence spectra of the hybrid NPs with the different FS/Ti molar ratios in PBS, and the integrated intensity changes with the NP concentration. The relationship between the luminescence intensity and FS content became completely opposite as compared to that observed in the atmospheric measurement. Namely, the luminescence intensity increases with the increasing NP concentration. The NPs with FS/Ti ratio = 1/100 exhibited the strongest luminescence centered at around 514 nm. Each luminescence spectrum has a broad shoulder at around 560 nm. As previously described, the luminescence at the 520 nm and the 560 nm shoulder can be attributed to the monomer dianion and the *J*-type aggregates, respectively. Taking into consideration that FS changes its form depending on the pK_a values as follows: cation to neutral (pK_a 2.1), neutral to monoanion (pK_a 4.2), and monoanion to dianion (pK_a 6.5).[53] It can be concluded that there existed both monomer dianions and *J*-type aggregates.[53,57,58] The luminescence efficiency of the monomer dianions is higher than that of the *J*-type aggregates, which is almost the same in this study, indicating that the relatively enhanced FS monomeric states in the PBS contribute to the present luminescence. However, it should be noted that there

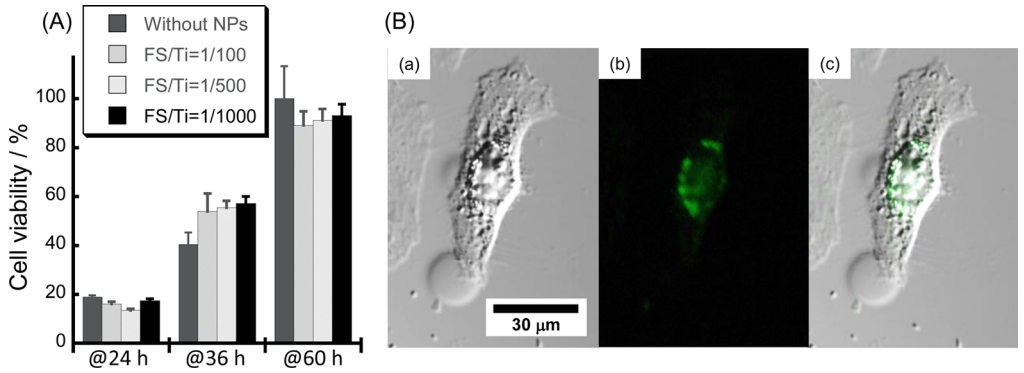

Figure 4. (A) Fibroblast viabilities of the additional culturing at 24, 36, and 60 h after adding the NPs. (B) (a) Differential interference, (b) fluorescent, and (c) the composite images from panels a and b of the fibroblast reacted with the NP with FS/Ti = 1/100 at the culture time of 24 h.

may be some contributions from the dissolved FS. Since there is another possibility that ODA dissolved, the exact amount of dissolved FS is now under investigation by various analytical techniques and will be reported in near future.

The possible reason for the different luminescence behaviors in air and in PBS can be explained on the basis of the number of water molecules accessible to the FS on/inside the hybrid surfaces (see Supporting Information Scheme S1). For the monomeric states of FS molecules on/inside the hybrid surfaces, water molecules, which work as luminescence quenching agents, can access the sample surfaces of the molar FS/Ti = 1/1000 easier than the case of the FS/Ti = 1/100. Taking into account that the ODA molecules can interact with a hydroxyl group of FS by hydrogen bonding on the hybrid surfaces and can be stabilized subsequently by the relatively week hydrophobic interactions among the ODA alkylchains in the case of FS/Ti = 1/100, the ODA molecules would prevent water molecules from accessing the FS, realizing more efficient luminescence in PBS. It is reported that the FS concentration of 1×10^{-4} M causes aggregate formation, while the FS concentration of 1×10^{-6} M does not result in any significant FS aggregation.[53,59] In the present case, the FS concentration was in the range from 1×10^{-4} to 1×10^{-3} (in Solution A (Table 1)), leading to the formation of aggregates and the more significant FS aggregation in the case of the FS/Ti = 1/100. The FS was diluted when solution A was admixed with solution B and also solution C, resulting in the final FS concentration of 2×10^{-5} to 2×10^{-4}. This indicates that FS molecules may be dissociated except for the sample with the molar FS/Ti = 1/100. In contrast, water molecules can access the dissociated and monomeric FS states on the sample surface with FS/Ti = 1/1000 more easily, although some FS molecules can be rearranged. For the measurements in air, the self-quenching in the aggregation state for the sample with the molar FS/Ti = 1/100 relatively affects the luminescence behavior. The amount of water molecules in air is extremely lower than those in PBS, thus the sample with the molar ratio of FS/Ti = 1/1000 did not suffer from quenching caused by the water molecules.

In Vitro Cytotoxicity of the Hybrid NPs. Figure 4A shows the cell viabilities of the fibroblasts cultured for 24, 36, and 60 h after adding the NPs on the adhered cell surfaces. The cells with and without adding the NPs significantly spread out on the plate and maintained their normal morphologies.[45] Furthermore, the proliferation behaviors by adding the NPs were almost the same as those without adding any NPs, indicating that the NPs are nontoxic. The size of the NPs is important for the cytotoxicity. For amorphous silica, the toxicity tends to be inversely related to the NP size, and a NP size below 100 nm has actually been found to induce the cytotoxicity.[20,60] It was also reported that titania NPs with the size of 25 nm induced a much greater inflammatory response to rats compared to larger particles with the size of 250 nm.[61] A number of previous studies have pointed out that the relationship between the size of NPs, cellular uptake and cytotoxicity is complicated. The uptake and cytotoxicity usually depends on many factors including composition, shape, surface state other than size, and even the type of cells. Among the various factors, smaller size should affect differently because surface area is getting larger when particle size decreases, resulting in higher surface energy. In this study, the NP size is ~400 nm, which would be a good candidate to exhibit a high cytocompatibility at least from a viewpoint of surface area.

Figure 4B shows differential interference, fluorescent, and the composite images of the fibroblast reacted with the NP with FS/Ti = 1/100 at the culture time of 24 h. The green luminescence was observed by the fluorescent microscopy. The fluorescent image indicates the presence of luminescent NPs located around the nuclei, and the cell would uptake the NPs, while the NPs were not functionalized with ligands which can promote the uptake so that the uptake behavior is not clear. With an increase in the culture time, the number of luminescent NPs in the cells increased. Thus, the NPs were found to be effectively taken up by the cell to show the cytocompatibility, and can be used as potential fluorescent labels in biomedical imaging.

As has described, NPs for biomedical applications should have stable/effective luminescent property and cytocompatibility. In this sense, tunable luminescence property and cytocomapatibility which we demonstrated in the present paper are promising for targeting, bioimaging and drug delivery. Furthermore, titania can effectively absorb light in UV region, allowing to protect FS molecules from degrading. The controllable particle size will be also helpful to systematically understand complicated behavior of the NPs in a human body.

CONCLUSIONS

We reported the synthesis of FS-containing monodispersed titania-octadecylamine hybrid spherical NPs and demonstrated their characteristic luminescence property and cytotocompatibility. The hybrid NPs were uniform in size and shape even if the molar FS/Ti ratio varied in the range from 1/1000 to 1/100, indicating that the alternative FS molecular states were confined in one nanoparticle. In addition to the formation

mechanism of the NPs, the origin of the characteristic luminescence was also discussed in detail; the luminescence can be controlled by varying the molar FS/Ti ratio, which is one possible factor that dominates the reversible monomeric/aggregation states of FS in various environments, such as in air and in PBS. The unique luminescence behavior will enable to determine a proper combination between material composition and an environment where they are used, being useful for various biomedical applications. We believe that a better understanding of the luminescence property and the cytocompatibility of nanomaterials contributes to the development of various multidisciplinary applications in such fields as biomedicine, optics and so on.

■ ASSOCIATED CONTENT

Ⓢ Supporting Information

Weight losses before and after the PBS treatment, ideal values calculated on the basis of the total amount of organic compounds in the starting solution, SEM image and the corresponding particle size distributions of the hybrid NPs with the FS/Ti molar ratio of 0, the optical and fluorescent microscope images, SEM images and the corresponding particle size distributions of the hybrid NPs synthesized under different flow rate of 1.5, 7.5, and 30 mL/min at the fixed parameters, SEM images and the corresponding particle size distributions of the hybrid NPs synthesized under the different H_2O/IPA molar ratio in the starting solution of 0.3/49.32, 1/61.65, and 3/61.65 at the fixed parameters, fluorescent microscope images and the luminescence intensities of the hybrid NPs with the different FS/Ti molar ratios of 1/1000, 1/500, and 1/100, TG−DTA curves of the hybrid NPs with the different FS/Ti molar ratios before and after the PBS treatment, and illustration of the possible FS molecular states on the titania-based hybrid NP surfaces. These materials are available free of charge via the Internet at http://pubs.acs.org.

■ AUTHOR INFORMATION

Corresponding Author

*E-mail: tagaya@mst.nagaokaut.ac.jp. Tel: +81-258-47-9345.

Notes

The authors declare no competing financial interest.

■ ACKNOWLEDGMENTS

This research was partially supported by the cosmetology research foundation, and further was partially supported by a Grant-in-Aid for the Adaptable and Seamless Technology Transfer Program through target-driven R&D (A-STEP No. AS251Z00303P) of the Japan Science and Technology Agency (JST).

■ REFERENCES

(1) Doane, T. L.; Burda, C. The unique role of nanoparticles in nanomedicine: Imaging, drug delivery, and therapy. *Chem. Soc. Rev.* **2012**, *41* (7), 2885−2911.

(2) Lee, D. E.; Koo, H.; Sun, I. C.; Ryu, J. H.; Kim, K.; Kwon, I. C. Multifunctional nanoparticles for multimodal imaging and theragnosis. *Chem. Soc. Rev.* **2012**, *41* (7), 2656−2672.

(3) Ogawa, M. Photoprocesses in mesoporous silicas prepared by a supramolecular templating approach. *J. Photochem. Photobiol., C* **2002**, *3* (2), 129−146.

(4) Sanchez, C.; Julian, B.; Belleville, P.; Popall, M. Applications of hybrid organic−inorganic nanocomposites. *J. Mater. Chem.* **2005**, *15* (35−36), 3559−3592.

(5) Sanchez, C.; Lebeau, B.; Chaput, F.; Boilot, J. P. Optical properties of functional hybrid organic−inorganic nanocomposites. *Adv. Mater.* **2003**, *15* (23), 1969−1994.

(6) Shiba, K.; Tagaya, M.; Tilley, R. D.; Hanagata, N. Oxide-based inorganic/organic and nanoporous spherical particles: Synthesis and functional properties. *Sci. Technol. Adv. Mater.* **2013**, *14*, 023002-1−023002-14.

(7) Beck, J. S.; Vartuli, J. C.; Roth, W. J.; Leonowicz, M. E.; Kresge, C. T.; Schmitt, K. D.; Chu, C. T. W.; Olson, D. H.; Sheppard, E. W.; McCullen, S. B.; Higgins, J. B.; Schlenker, J. L. A new family of mesoporous molecular-sieves prepared with liquid-crystal templates. *J. Am. Chem. Soc.* **1992**, *114* (27), 10834−10843.

(8) Hoppe, R.; Ortlam, A.; Rathousky, J.; SchulzEkloff, G.; Zukal, A. Synthesis of titanium-containing MCM-41 mesoporous molecular sieves in the presence of zinc phthalocyanine and rhodamine B. *Microporous Mater.* **1997**, *8* (5−6), 267−273.

(9) Huang, M. H.; Dunn, B. S.; Soyez, H.; Zink, J. I. In situ probing by fluorescence spectroscopy of the formation of continuous highly-ordered lamellar-phase mesostructured thin films. *Langmuir* **1998**, *14* (26), 7331−7333.

(10) Marlow, F.; McGehee, M. D.; Zhao, D. Y.; Chmelka, B. F.; Stucky, G. D. Doped mesoporous silica fibers: A new laser material. *Adv. Mater.* **1999**, *11* (8), 632−636.

(11) Ogawa, M.; Igarashi, T.; Kuroda, K. Thermotropic behavior of the silica-alkyltrimethylammonium chloride mesostructured materials. *Chem. Mater.* **1998**, *10* (5), 1382−1385.

(12) Tagaya, M.; Motozuka, S.; Kobayashi, T.; Ikoma, T.; Tanaka, J. Efficient incorporation of monomeric anthracene into nanoporous silica/surfactant nanocomposite spheres using a mechanochemical solid state reaction. *J. Mater. Chem.* **2012**, *22* (36), 18741−18743.

(13) Zhou, H. S.; Honma, I. Synthesis of chlorophyll doped silica-mesostructure materials. *Chem. Lett.* **1998**, *10*, 973−974.

(14) Tagaya, M.; Hanagata, N.; Kobayashi, T. Templating effect of mesostructured surfactant-silica monolithic films on the surface structural and mechanical properties. *ACS Appl. Mater. Interfaces* **2012**, *4* (11), 6169−6175.

(15) Kumar, R.; Roy, I.; Hulchanskyy, T. Y.; Goswami, L. N.; Bonoiu, A. C.; Bergey, E. J.; Tramposch, K. M.; Maitra, A.; Prasad, P. N. Covalently dye-linked, surface-controlled, and bioconjugated organically modified silica nanoparticles as targeted probes for optical imaging. *ACS Nano* **2008**, *2* (3), 449−456.

(16) Tagaya, M.; Ogawa, M. Possible pore size effects on the state of tris(8-quinolinato) aluminum(III) (Alq_3) adsorbed in mesoporous silicas and their temperature dependence. *Phys. Chem. Chem. Phys.* **2008**, *10* (45), 6849−6855.

(17) Tagaya, M.; Ogawa, M. Luminescence of tris(8-quinolinato)-aluminum(III) (Alq_3) adsorbed into mesoporous silica. *Chem. Lett.* **2006**, *35* (1), 108−109.

(18) Bardi, G.; Malvindi, M. A.; Gherardini, L.; Costa, M.; Pompa, P. P.; Cingolani, R.; Pizzorusso, T. The biocompatibility of amino functionalized CdSe/ZnS quantum-dot-doped SiO_2 nanoparticles with primary neural cells and their gene carrying performance. *Biomaterials* **2010**, *31* (25), 6555−6566.

(19) Han, R. C.; Yu, M.; Zheng, Q.; Wang, L. J.; Hong, Y. K.; Sha, Y. L. A facile synthesis of small-sized, highly photoluminescent, and monodisperse CdSeS QD/SiO_2 for live cell imaging. *Langmuir* **2009**, *25* (20), 12250−12255.

(20) Tagaya, M.; Hanagata, N.; Ikoma, T.; Kobayashi, T.; Shiba, K.; Yoshioka, T.; Tanaka, J. Cytotoxicity and cancer detection ability of the luminescent nanoporous silica spheres immobilized with folic acid derivative. *Key Eng. Mater.* **2013**, *529−530*, 630−635.

(21) Tagaya, M.; Ikoma, T.; Yoshioka, T.; Motozuka, S.; Minami, F.; Tanaka, J. Efficient synthesis of Eu(III)-containing nanoporous silicas. *Mater. Lett.* **2011**, *65* (14), 2287−2290.

(22) Tagaya, M.; Ikoma, T.; Yoshioka, T.; Motozuka, S.; Xu, Z. F.; Minami, F.; Tanaka, J. Synthesis and luminescence properties of Eu(III)-doped nanoporous silica spheres. *J. Colloid Interface Sci.* **2011**, *363* (2), 456−464.

(23) Tagaya, M.; Ikoma, T.; Yoshioka, T.; Xu, Z. F.; Tanaka, J. Immobilization of folic acid on Eu^{3+}-doped nanoporous silica spheres. *Chem. Commun.* **2011**, *47* (29), 8430−8432.
(24) Yang, P. P.; Quan, Z. W.; Lu, L. L.; Huang, S. S.; Lin, J. Luminescence functionalization of mesoporous silica with different morphologies and applications as drug delivery systems. *Biomaterials* **2008**, *29* (6), 692−702.
(25) Chen, D. H.; Cao, L.; Huang, F. Z.; Imperia, P.; Cheng, Y. B.; Caruso, R. A. Synthesis of monodisperse mesoporous titania beads with controllable diameter, high surface areas, and variable pore diameters (14−23 nm). *J. Am. Chem. Soc.* **2010**, *132* (12), 4438−4444.
(26) Eiden-Assmann, S.; Widoniak, J.; Maret, G. Synthesis and characterization of porous and nonporous monodisperse colloidal TiO_2 particles. *Chem. Mater.* **2004**, *16* (1), 6−11.
(27) Han, X. G.; Kuang, Q.; Jin, M. S.; Xie, Z. X.; Zheng, L. S. Synthesis of titania nanosheets with a high percentage of exposed (001) facets and related photocatalytic properties. *J. Am. Chem. Soc.* **2009**, *131* (9), 3152−3153.
(28) Hong, M. P.; Kim, J. Y.; Vemula, K.; Kim, H. S.; Yoon, K. B. Synthesis of monodisperse mesoporous TiO_2 spheres with tunable sizes between 0.6 and 3.1 μm and effects of reaction temperature, Ti source purity, and type of alkylamine on size and monodispersity. *Chem. Commun.* **2012**, *48* (35), 4250−4252.
(29) Shrestha, N. K.; Macak, J. M.; Schmidt-Stein, F.; Hahn, R.; Mierke, C. T.; Fabry, B.; Schmuki, P. Magnetically guided titania nanotubes for site-selective photocatalysis and drug release. *Angew. Chem., Int. Ed. Engl.* **2009**, *48* (5), 969−972.
(30) Yang, H. G.; Sun, C. H.; Qiao, S. Z.; Zou, J.; Liu, G.; Smith, S. C.; Cheng, H. M.; Lu, G. Q. Anatase TiO_2 single crystals with a large percentage of reactive facets. *Nature* **2008**, *453* (7195), 638−641.
(31) Crepaldi, E. L.; Soler-Illia, G.; Grosso, D.; Cagnol, F.; Ribot, F.; Sanchez, C. Controlled formation of highly organized mesoporous titania thin films: From mesostructured hybrids to mesoporous nanoanatase TiO_2. *J. Am. Chem. Soc.* **2003**, *125* (32), 9770−9786.
(32) Shiba, K.; Sato, S.; Ogawa, M. Preparation of well-defined titania-silica spherical particles. *J. Mater. Chem.* **2012**, *22* (19), 9963−9969.
(33) Wu, C. W.; Ohsuna, T.; Kuwabara, M.; Kuroda, K. Formation of highly ordered mesoporous titania films consisting of crystalline nanopillars with inverse mesospace by structural transformation. *J. Am. Chem. Soc.* **2006**, *128* (14), 4544−4545.
(34) Yoshitake, H.; Sugihara, T.; Tatsumi, T. Preparation of wormhole-like mesoporous TiO_2 with an extremely large surface area and stabilization of its surface by chemical vapor deposition. *Chem. Mater.* **2002**, *14* (3), 1023−1029.
(35) Bergeron, B. V.; Meyer, G. J. Reductive electron transfer quenching of MLCT excited states bound to nanostructured metal oxide thin films. *J. Phys. Chem. B* **2003**, *107* (1), 245−254.
(36) Qin, W. P.; Zhang, D. S.; Zhao, D.; Wang, L. L.; Zheng, K. Z. Near-infrared photocatalysis based on YF_3: Yb^{3+}, Tm^{3+}/TiO_2 core/shell nanoparticles. *Chem. Commun.* **2010**, *46* (13), 2304−2306.
(37) Wu, K. C. W.; Yamauchi, Y.; Hong, C. Y.; Yang, Y. H.; Liang, Y. H.; Funatsu, T.; Tsunoda, M. Biocompatible, surface functionalized mesoporous titania nanoparticles for intracellular imaging and anticancer drug delivery. *Chem. Commun.* **2011**, *47* (18), 5232−5234.
(38) Yin, J. B.; Xiang, L. Q.; Zhao, X. P. Monodisperse spherical mesoporous Eu-doped TiO_2 phosphor particles and the luminescence properties. *Appl. Phys. Lett.* **2007**, *90* (11), 113112-1−113112-3.
(39) Lamer, V. K.; Dinegar, R. H. Theory, production and mechanism of formation of monodispersed hydrosols. *J. Am. Chem. Soc.* **1950**, *72* (11), 4847−4854.
(40) Park, J.; Privman, V.; Matijevic, E. Model of formation of monodispersed colloids. *J. Phys. Chem. B* **2001**, *105* (47), 11630−11635.
(41) Zaiser, E. M.; Lamer, V. K. The kinetics of the formation and growth of monodispersed sulfur hydrosols. *J. Colloid Sci.* **1948**, *3* (6), 571−598.
(42) Shiba, K.; Ogawa, M. Microfluidic syntheses of well-defined submicron nanoporous titania spherical particles. *Chem. Commun.* **2009**, *44*, 6851−6853.
(43) Shiba, K.; Onaka, K.; Ogawa, M. Preparation of mono-dispersed titanium oxide-octadecylamine hybrid spherical particles in the submicron size range. *RSC Adv.* **2012**, *2* (4), 1343−1349.
(44) Tominaga, H.; Ishiyama, M.; Ohseto, F.; Sasamoto, K.; Hamamoto, T.; Suzuki, K.; Watanabe, M. A water-soluble tetrazolium salt useful for colorimetric cell viability assay. *Anal. Commun.* **1999**, *36* (2), 47−50.
(45) Tagaya, M.; Ikoma, T.; Takemura, T.; Migita, S.; Okuda, M.; Yoshioka, T.; Hanagata, N.; Tanaka, J. Initial Adhesion behavior of fibroblasts onto hydroxyapatite nanocrystals. *Bioceram. Dev. Appl.* **2011**, *1*, 110165-1−110165-4.
(46) Okuda, M.; Takeguchi, M.; Zhu, Y. F.; Hashimoto, A.; Ogawa, N.; Tagaya, M.; Chen, S.; Hanagata, N.; Ikoma, T. Structural analysis of rattle-type hollow mesoporous silica spheres using electron tomography and energy filtered imaging. *Surf. Interface Anal.* **2010**, *42* (10−11), 1548−1551.
(47) Shiba, K.; Sato, S.; Ogawa, M. Preparation of monodispersed spherical titania-octadecylamine particles containing silane-coupling reagents. *Bull. Chem. Soc. Jpn.* **2012**, *85* (9), 1040−1047.
(48) Ichinose, I.; Kunitake, T. Molecular wrapping of a fluorescent dye with TiO_2-gel and capping reagents. *Chem. Lett.* **2001**, *7*, 626−627.
(49) Foster, A. S.; Nieminen, R. M. Adsorption of acetic and trifluoroacetic acid on the TiO_2(110) surface. *J. Chem. Phys.* **2004**, *121* (18), 9039−9042.
(50) Gratzel, M. Solar energy conversion by dye-sensitized photovoltaic cells. *Inorg. Chem.* **2005**, *44* (20), 6841−6851.
(51) Song, X. M.; Zhao, Y. L.; Wang, H. T.; Do, Q. G. Fabrication of polymer microspheres using titania as a photocatalyst and pickering stabilizer. *Langmuir* **2009**, *25* (8), 4443−4449.
(52) Wang, Y. D.; Ma, C. L.; Sun, X. D.; Li, H. D. Synthesis and characterization of mesoporous TiO_2 with wormhole-like framework structure. *Appl. Catal., A* **2003**, *246* (1), 161−170.
(53) De, S.; Kundu, R. Spectroscopic studies with fluorescein dye-protonation, aggregation, and interaction with nanoparticles. *J. Photochem. Photobiol., A* **2011**, *223* (2−3), 71−81.
(54) Fujii, T.; Ishii, A.; Takusagawa, N.; Anpo, M. Fluorescence-spectra and chemical-species of fluorescein molecules adsorbed on a calcinated porous vycor glass. *Res. Chem. Intermed.* **1992**, *17* (1), 1−14.
(55) Jalkanen, P.; Kulju, S.; Arutyunov, K.; Antila, L.; Myllyperkio, P.; Ihalainen, T.; Kaariainen, T.; Kaariainen, M. L.; Korppi-Tommola, J. Fabrication and characterization of vacuum deposited fluorescein thin films. *Thin Solid Films* **2011**, *519* (11), 3835−3839.
(56) Das, S.; Chattopadhyay, A. P.; De, S. Controlling J aggregation in fluorescein by bile salt hydrogels. *J. Photochem. Photobiol., A* **2008**, *197* (2−3), 402−414.
(57) Sjöback, R.; Nygren, J.; Kubista, M. Absorption and fluorescence properties of fluorescein. *Spectrochim. Acta, Part A* **1995**, *51* (6), L7−L21.
(58) Zhao, Z.-G.; Shen, T.; Xu, H.-J. The absorption and structure of fluorescein and its ethyl derivatives in various solutions. *Spectrochim. Acta, Part A* **1989**, *45* (11), 1113−1116.
(59) De, S.; Das, S.; Girigoswami, A. Environmental effects on the aggregation of some xanthene dyes used in lasers. *Spectrochim. Acta, Part A* **2005**, *61* (8), 1821−1833.
(60) Yu, K. O.; Grabinski, C. M.; Schrand, A. M.; Murdock, R. C.; Wang, W.; Gu, B. H.; Schlager, J. J.; Hussain, S. M. Toxicity of amorphous silica nanoparticles in mouse keratinocytes. *J. Nanopart. Res.* **2009**, *11* (1), 15−24.
(61) Oberdorster, G.; Ferin, J.; Lehnert, B. E. Correlation between particle-size, in-vivo particle persistence, and lung injury. *Environ. Health Perspect.* **1994**, *102*, 173−179.

NOTE ADDED AFTER ASAP PUBLICATION

This paper was published on the Web on April 25, 2014, with errors in the Title of the paper. The corrected version was reposted on April 28, 2014.